Flagellar Motor Switching in Caulobacter Crescentus Obeys First Passage Time Statistics

Michael Morse, Jordan Bell, Guanglai Li, and Jay X. Tang

Phys. Rev. Lett. **115**, 198103 — Published 5 November 2015

DOI: 10.1103/PhysRevLett.115.198103

Flagellar Motor Switching in *Caulobacter Crescentus is a First Passage Time Process*

Michael Morse, Jordan Bell, Guanglai Li, and Jay X. Tang*

Physics Department, Brown University, Providence RI

(Dated: October 14, 2015)

Abstract

A *Caulobacter crescentus* swarmer cell is propelled by a helical flagellum, which is rotated by a motor at its base. The motor alternates between rotating in the clockwise and counterclockwise directions and spends variable intervals of time in each state. We measured the distributions of these intervals for cells either free-swimming or tethered to a glass slide. A peak time of around one second is observed in the distributions for both motor directions with counterclockwise intervals more sharply peaked and clockwise intervals displaying a larger tail at long times. We show that distributions of rotation intervals fit first passage time statistics for a biased random walker and the dynamic binding of CheY-P to FliM motor subunits accounts for this behavior. Our results also suggest that the presence of multiple CheY proteins in *C. crescentus* may be responsible for differences between its switching behavior and that of the extensively studied *E. coli*.

Bacterial flagellar motors rotate helical flagella to propel cells through their fluid environment. The direction in which the motor rotates and the time intervals between switches in rotation direction determine the cell's trajectory. For uni-flagellated bacteria, a cell swims forward as a pusher or backward as a puller [1] depending on rotation direction. Specifically for *C. crescentus*, since its flagellum is a right-handed helix [2], the cell swims forward/backward when its flagellar motor rotates clockwise/counterclockwise (CW/CCW). The motor of *C. crescentus* has a high CW bias, i.e., the fraction of time spent rotating in the CW direction is greater than 0.5. CW intervals, on average, are longer than CCW intervals. Since the forward and backward free swimming speeds are roughly equal [3], greater CW bias results in greater displacements during forward swimming.

There has been recent debate as to how the intervals between motor switches are distributed. An equilibrium model of the flagellar motor, in which it switches between the CW and CCW states at constant rates, would produce exponentially decaying distributions [4]. In contrast, a distribution peaked above zero seconds would require a more complex switching mechanism [4, 5]. For *E. coli*, both exponentially decaying and peaked distributions have been reported [5–11]. A peaked distribution has recently been observed for uni-flagellated *Vibrio alginolyticus* [12]. In this study, we measure the distribution of intervals of both CW and CCW rotation for *C. crescentus* by observing cells either tethered to a glass slide or free-swimming. We compare the results from these two experiments to check for artifacts or biases introduced by either method.

Cells attached to a glass slide were imaged at 60X magnification using phase contrast and recorded at 30 frames per second (see supplemental material IV for detailed materials and methods). The length of CW and CCW rotation intervals were measured by marking frames where the cell body and motor switch rotation direction. To compensate for the short lifetime of the motile swarmer phase, which can end prematurely due to physical effects of tethering [13], a total of 36 cells were observed. Whereas large cell to cell variability has been observed in clonal populations of *E. coli* [14], only small deviations in CW bias were

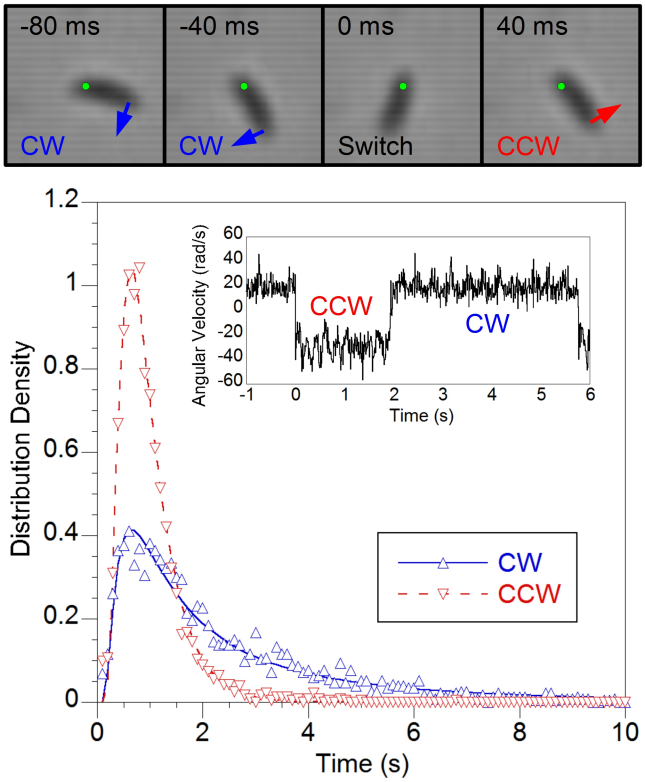

FIG. 1. Distributions of motor rotation intervals for tethered cells. Top: Cell body rotating around a fixed point (green dot) with the direction of rotation noted by an arrow. A switch from CW to CCW rotation occurs at time 0 ms. Bottom: Distribution density of motor rotation intervals for both directions plotted along with fit lines to first passage time theory. Inset: The angular velocity of a rotating cell over a short duration showing a pair of CW and CCW intervals. Angular velocity is nearly constant during rotation intervals and quickly switches sign when the motor switches direction. A total of 2338 CW and 2236 CCW intervals were recorded (supplemental video 1).

observed in our sample (supplemental material I). Distributions of CW and CCW rotation intervals were created using data pooled from all cells. For both directions, the distributions peak slightly under one second and decay at longer times (fig 1). The CCW distribution is more sharply peaked whereas the CW distribution decays more slowly at longer times such that the average interval is 2.5 times that of CCW rotation. Distributions of intervals created from single cell data also show these patterns, but with more noise due to small sample size (supplemental fig S2).

Free swimming cells were imaged at 10X magnification using darkfield. Swimming trajectories were observed over a 1 mm field of view in a thin sample to minimize measurement bias

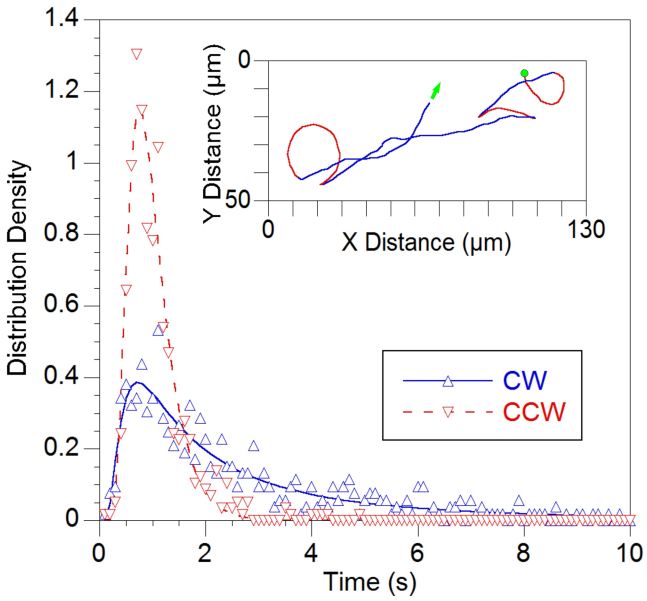

FIG. 2. Distribution of motor rotation intervals for free-swimming cells along with fit lines to first passage time theory. Both distributions agree with results from tethered cells. Inset: Sample trajectory of a cell with forward (CW) and backward (CCW) swimming segments drawn as blue and red lines, respectively. The green dot and arrow mark the beginning and end of the trajectory, respectively. A total of 525 CW and 575 CCW intervals were recorded (supplemental video 2).

against long rotation intervals. Frames in which cell swimming and motor rotation switched direction were marked. Aided by differences between forward (CW) and backward (CCW) swimming, in particular the handedness of circular trajectories near the sample's surfaces and a reorientation event at the start of foward swimming, referred to as a flick [12, 15], motor rotation direction was determined for every interval. Combining data from 100 trajectories yielded distributions similar to those of tethered cells (fig 2).

The distributions observed using both techniques are clearly peaked near one second, indicating that motor switching is not an equilibrium process and violates detailed balance [4]. The distributions do, however, closely follow fit lines produced by first passage time theory for a biased random walker.

$$P(t) = \frac{x}{\sqrt{4\pi D t^3}} e^{\frac{-(x-vt)^2}{4Dt}} \tag{1}$$

where $P(t)$ is the probability of a random walker passing a threshold a given distance x away from its starting position at time t, given a diffusion constant D and an underlying bias v

	CW(T)	CW(FS)	CCW (T)	CCW(FS)
A Best Fit	2.0	2.3	3.3	5.4
B Best Fit	3.0	3.1	0.97	0.99
R Squared	0.96	0.88	0.99	0.96

TABLE I. First passage time fit parameters for tethered (T) and free-swimming (FS) cells. B is 3 times larger for CW than CCW rotation whereas A is slightly larger for CCW rotation.

(a constant drift velocity) [16]. We reparametrize this expression using two independent parameters,

$$P(t) = \sqrt{\frac{A}{2\pi t^3}} e^{\frac{-A}{2t}(1-\frac{t}{B})^2} \tag{2}$$

where $A = \frac{x^2}{2D}$ and $B = \frac{x}{v}$, both with units of time. A, a measure of diffusivity, is the time at which the walker's root mean squared displacement due to diffusion is equal to the distance between the starting position and the threshold. B, a measure of bias, is the time required to reach the threshold from the start position moving at the bias velocity. This distribution is also known as an inverse Gaussian, where B is the mean and A is the shape parameter.

We found the best fit parameters for both sets of data (table 1). B is, as expected, approximately equal to the average interval time and significantly larger for CW rotation. A is slightly larger for CCW rotation than CW but less consistent between the two experiments. Changing the value of A within this range, however, alters the fit line to a much lesser degree compared with changing the value of B, which has excellent agreement between the two experiments. We suspect the discrepancy in A values may be due to noise. The agreement between the free-swimming and tethered cells also indicates that the motor switching mechanism is not dramatically altered by the load on the motor and the resulting decrease in rotation speed. This contrasts with experiments using *E. coli* that show motor switching rates vary with rotational speed [7, 17].

To understand why motor rotation intervals exhibit first passage time behavior, we seek a model based on the structure of the motor and recent models of allosteric response [18, 19]. Motor switching is controlled by the C-ring, a structure composed of proteins FliM, FliN, and FliG. There are approximately 34 FliM subunits in the C-ring [20, 21]. Each subunit can be

in either CW or CCW conformation, but with a significant energy cost for adjacent subunits existing in opposing conformations [18, 19]. It is most energetically favorable for all subunits to be in the same conformation, resulting in motor rotation in the corresponding direction. In order for the C-ring to switch between CW and CCW conformations, one or more subunits must initially switch to oppose the others with their neighbors quickly doing the same until all subunits have flipped into the new conformation. Recent work suggests that this process occurs on the order of tens of milliseconds [22]. During second(s)-long rotation intervals, individual subunits can be taken to be in mostly congruous arrangement. Subunits can also be bound by CheY-P, the phosphorylated form of signaling protein CheY [23]. It is well established that CheY-P regulates motor switching behavior and chemotaxis [24]. Thus, every subunit can be in one of four states, CW or CCW conformation in combination with CheY-P bound or unbound. Depending on a subunit's directional conformation, there is an energetic cost or saving from CheY-P binding (fig 3A). Bound subunits minimize their energy state by switching to the CW conformation while the reverse is true for unbound subunits [25]. Each subunit can independently bind and unbind such that the total number of bound subunits in the C-ring varies over time (fig 3B). The C-ring as a whole has two semi-stable states, with all subunits in either CW or CCW conformation. The energy levels of these states depend on the number of CheY-P bound subunits (fig 3C) [26]. As more subunits are CheY-P bound, the energy of the CW state decreases while that of the CCW state increases and vice versa. We should note that two competing models have also been recently proposed, based on experiments on *E. coli*, in which switching rate varies due to fluctuations in CheY-P concentration [8] or due to increased mechanical load on the motor [9]. These alternative models, however, can not be reconciled with our observations of *C. crescentus* (supplemental material III).

Focusing on the binding of CheY-P to individual FliM subunits, we build a simple model that explains the biased random walk behavior seen in our experiments. We define the variable n as the total number of subunits with CheY-P bound at a given time, such that there are $(34 - n)$ subunits unbound. As individual subunits independently become bound or unbound, n fluctuates between 0 and 34. Over time, individual subunits will bind to CheY-P at some rate Ck_{on}, which is directly proportional to the concentration of CheY-P, and unbind at some rate k_{off}. We expect Ck_{on} to remain constant in our experiments as the cells do not experience any chemical gradients. These rates will differ for (un)binding to

FliM subunits in CW or CCW conformation due to CheY-P's different affinity for each. We also define switching rates between CW and CCW rotations using the common assumption that the rates are proportional to the exponential of the energy difference between the states (see supplemental material II for detailed math). For values of E on the order of k_BT, these rates increase drastically above and below $n = 17$, respectively. The probability that a switch occurs in a small time step dt quickly transitions from near zero to one once n is sufficiently large or small (fig 3D). The values of n that enable switching act as the thresholds for a first passage time random walk. A CW rotation interval begins when n is large and ends when n is small. The time required for this process is dictated by random binding and unbinding of individual FliM subunits (fig 3E).

The mean B and shape parameter A of the curves produced by this model depend on the (un)binding rates and energy of CheY-P to FliM. In particular, the diffusion timescale, A, decreases as the (un)binding rates increase, whereas the bias timescale, B, depends on the difference between the two rates. Solving for the exact relationship between these parameters is complicated by variable instantaneous bias in the n random walk (see supplemental material II). Incremental adjustments of the (un)binding rates, however, can lead to a parameter set that reproduces the distributions seen in our experiments.

While our model is based primarily on extensively studied *E. coli*, motor structure is mostly conserved among many bacterial species. Our data, however, suggests that *C. crescentus* motor switching must differ from that of *E. coli* in one key manner. The first passage time fit yields a significant bias towards the switching threshold (B is positive) for both CW and CCW intervals. This is not possible in a single CheY-P system, as in *E. coli*, for which the conformational spread model produces near exponential rotation interval distributions [22]. *C. crescentus*, however, expresses multiple CheY proteins. Their exact roles in chemotaxis and motility are not currently known. They may exist in different concentrations within the cell and have different binding affinities to FliM. Complex interactions could also exist, including cooperative and competitive binding. To test how such interactions impact motor rotation, we simulate a system in which two different CheY molecules are present. The first acts like the single CheY of *E. coli*. For reference, experiments on *E. coli* have found binding rates on the order of 10 s^{-1} [27, 28] and simulations of the allosteric regulation model have suggested a binding energy of $\sim$1 k_BT [22]. The second CheY has negligible binding energy, but it competitively binds to CW conformation FliM. This simple

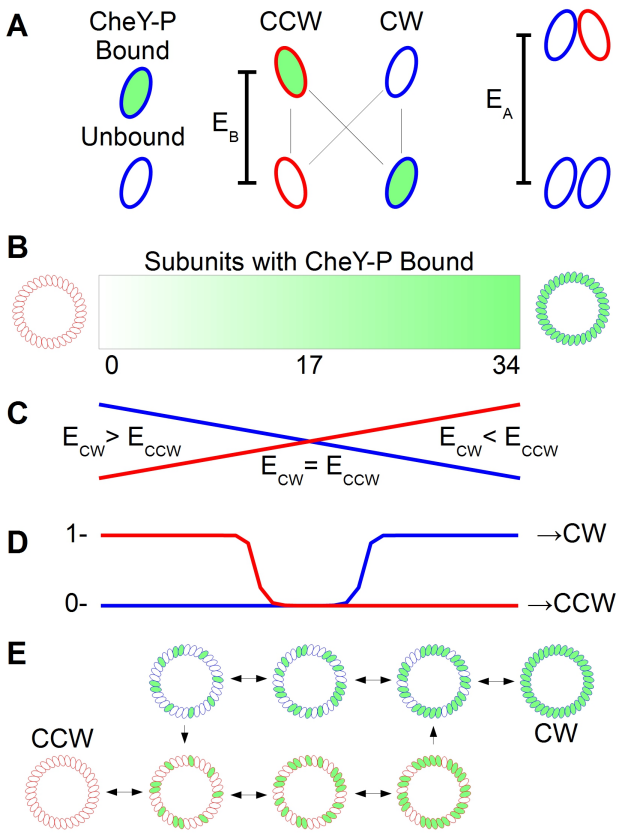

FIG. 3. Schematic illustration of conformation and binding states of FliM subunits in the C-ring. (A) Individual FliM subunits can be in either CW or CCW conformation and either CheY-P bound or unbound. Subunits in CCW conformation are at higher energy when bound whereas the reverse is true for subunits in CW conformation. There is a large energy cost for adjacent subunits in opposing conformations [18]. (B) The number of subunits with CheY-P bound performs a random walk between 0 and 34 according to rates of binding and unbinding. (C) The C-ring occupies one of two energy states corresponding to CW and CCW rotation with all subunits locked in the same conformation. The CW state lowers its energy level compared to the CCW state as the number of bound subunits increases, promoting switching from CCW to CW rotation. Decreasing the number of bound subunits has the opposite effect and promotes switching from CW to CCW rotation. (D) The probility of a motor switch occuring in a small timestep jumps for near 0 to 1 once the energy states become sufficiently unbalanced. (E) Individual subunits bind or unbind to CheY-P over time, and the C-ring switches conformation when a threshold is reached. The system continuously follows this loop and the time required to reach one threshold when starting from the other determines the length of a rotation interval.

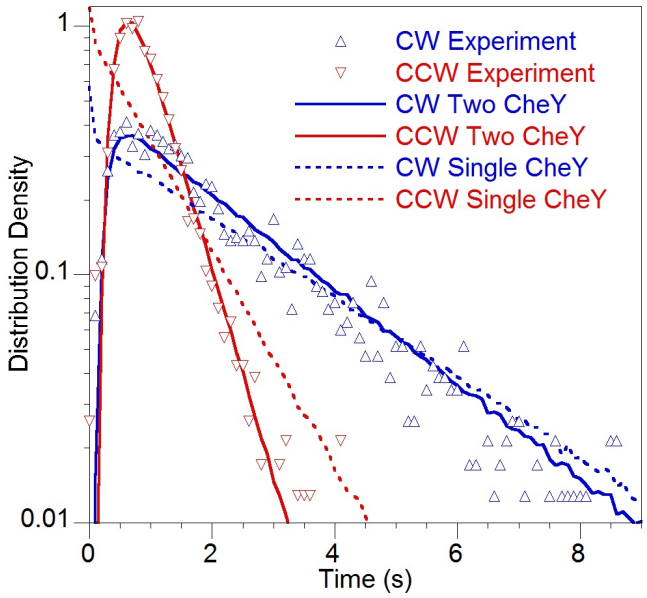

FIG. 4. Distributions of simulated motor rotation intervals using a single CheY-P (dashed lines) or two competitively binding CheY-P molecules (solid lines). When simulation parameters are adjusted so that average interval length matches experimental values, only the competitively binding scheme can produce the peaked distributions that match our experimental results (triangles). 1 million intervals were simulated for each curve.

model can be exactly fit to our experimental data, while a single CheY-P system can not (fig 4). While many schemes invoking a multitude of CheY-P interactions are possible and this particular fit is not unique, this example does suggest that interactions between multiple CheY molecules can account for *C. crescentus* switching behavior.

While our experiments observed cells at equilibrium behavior, our model can also account for the chemotactic response of a cell. While k_{off} is constant, changing levels of CheY-P induced by the cell's chemical sensing processes will change the value of Ck_{on}, thereby altering the average length of rotation intervals. As CheY-P concentration increases, the value of B will simultaneously increase for CW rotation and decrease for CCW rotation, resulting longer CW intervals and shorter CCW intervals. The model captures these results correctly as CW bias displays a sigmoidal form as a function of CheY-P concentration (supplemental fig s4). Distinctively, changing CheY-P levels do not simply shift the distribution's peak position to achieve a new average time. Instead, the relative prominence of the peak versus the tail is altered. Future measurements under chemotactic conditions can test for this

effect.

The peaked distributions of motor rotation intervals have a large impact on the motility of *C. crescentus*, as rotation time determines swimming distance. Since uni-flagellated swimmers follow a "run-reverse-flick" swimming pattern [12, 15] dissimilar to the "run-tumble" behavior of multi-flagellated swimmers [29], their switching behavior may have evolved differently. Notably for uni-flagellated swimmers, forward swimming is always followed by backward swimming and the net displacement over each complete cycle is proportional to the difference in CW and CCW rotation times. Additionally, uni-flagellated swimmers travel in circular trajectories of varying handedness and radius near different surfaces [30, 31] such that rotation intervals determine reorientation. The effects of peaked interval distributions may be particualrly relevant to the ability of cells to explore their environments, navigate chemical gradients, and perform other biological functions [32].

We acknowledge support of this work by NSF Grants PHY 1058375 and CBET 1438033. We thank Y. Brun of Indiana University for the bacterial strain used in the study.

* Jay˙Tang@Brown.edu

[1] K. Drescher, J. Dunkel, L. H. Cisneros, S. Ganguly, and R. E. Goldstein, Proceedings of the National Academy of Sciences **108**, 10940 (2011).

[2] S. Koyasu and Y. Shirakihara, Journal of molecular biology **173**, 125 (1984).

[3] B. Liu, M. Gulino, M. Morse, J. X. Tang, T. R. Powers, and K. S. Breuer, Proceedings of the National Academy of Sciences **111**, 11252 (2014).

[4] Y. Tu, Proceedings of the National Academy of Sciences **105**, 11737 (2008).

[5] E. A. Korobkova, T. Emonet, H. Park, and P. Cluzel, Physical review letters **96**, 058105 (2006).

[6] S. M. Block, J. E. Segall, and H. C. Berg, Journal of bacteriology **154**, 312 (1983).

[7] K. A. Fahrner, W. S. Ryu, and H. C. Berg, Nature **423**, 938 (2003).

[8] E. Korobkova, T. Emonet, J. M. Vilar, T. S. Shimizu, and P. Cluzel, Nature **428**, 574 (2004).

[9] S. B. van Albada, S. Tănase-Nicola, and P. R. ten Wolde, Molecular systems biology **5** (2009).

[10] H. Park, P. Oikonomou, C. C. Guet, and P. Cluzel, Biophysical journal **101**, 2336 (2011).

[11] F. Wang, J. Yuan, and H. C. Berg, Proceedings of the National Academy of Sciences **111**,

15752 (2014).

[12] L. Xie, T. Altindal, S. Chattopadhyay, and X.-L. Wu, Proceedings of the National Academy of Sciences **108**, 2246 (2011).

[13] G. Li, P. J. Brown, J. X. Tang, J. Xu, E. M. Quardokus, C. Fuqua, and Y. V. Brun, Molecular microbiology **83**, 41 (2012).

[14] J. L. Spudich, D. Koshland Jr, *et al.*, Nature **262**, 467 (1976).

[15] K. Son, J. S. Guasto, and R. Stocker, Nature Physics **9**, 494 (2013).

[16] S. Redner, *A guide to first-passage processes* (Cambridge University Press, 2001).

[17] S. Khan and R. M. Macnab, Journal of molecular biology **138**, 563 (1980).

[18] T. Duke, N. Le Novere, and D. Bray, Journal of molecular biology **308**, 541 (2001).

[19] D. Bray and T. Duke, Annu. Rev. Biophys. Biomol. Struct. **33**, 53 (2004).

[20] D. R. Thomas, D. G. Morgan, and D. J. DeRosier, Proceedings of the National Academy of Sciences **96**, 10134 (1999).

[21] H. S. Young, H. Dang, Y. Lai, D. J. DeRosier, and S. Khan, Biophysical journal **84**, 571 (2003).

[22] F. Bai, R. W. Branch, D. V. Nicolau, T. Pilizota, B. C. Steel, P. K. Maini, and R. M. Berry, Science **327**, 685 (2010).

[23] M. Welch, K. Oosawa, S.-l. Aizawa, and M. Eisenbach, Proceedings of the National Academy of Sciences **90**, 8787 (1993).

[24] P. Cluzel, M. Surette, and S. Leibler, Science **287**, 1652 (2000).

[25] B. E. Scharf, K. A. Fahrner, L. Turner, and H. C. Berg, Proceedings of the National Academy of Sciences **95**, 201 (1998).

[26] A. Mogilner, T. C. Elston, H. Wang, and G. Oster, in *Computational cell biology* (Springer, 2002) pp. 320–353.

[27] V. Sourjik and H. C. Berg, Proceedings of the National Academy of Sciences **99**, 12669 (2002).

[28] Y. Sagi, S. Khan, and M. Eisenbach, Journal of Biological Chemistry **278**, 25867 (2003).

[29] H. C. Berg, *E. coli in Motion* (Springer Science & Business Media, 2004).

[30] G. Li, L.-K. Tam, and J. X. Tang, Proceedings of the National Academy of Sciences **105**, 18355 (2008).

[31] M. Morse, A. Huang, G. Li, M. R. Maxey, and J. X. Tang, Biophysical journal **105**, 21 (2013).

[32] Y. Yang, J. He, T. Altindal, L. Xie, and X.-L. Wu, Biophysical journal **109**, 1058 (2015).